18th International Conference on Structural Mechanics in Reactor Technology (SMiRT 18)
Beijing, China, August 7-12, 2005
SMiRT18-B03-2

CHANGE-SCALE MODELLING OF THE THERMOMECHANICAL BEHAVIOUR OF PARTICLE-BASED NUCLEAR FUEL ASSEMBLIES

Serge PASCAL
CEA/DEN/DM2S/SEMT/LM2S
CEN Saclay
91191 Gif-sur-Yvette
Phone: (+33).1.69.08.61.37, Fax: (+33).1.69.08.86.84
E-mail: serge.pascal@cea.fr

ABSTRACT

In the frame of the developments carried out by the CEA on High Temperature Reactors or Gas-cooled Fast Reactors of 4th generation, we propose a modelling of the thermomechanical behaviour of particle-based nuclear fuel composites on the basis of the "n-layered inclusion-based self-consistent scheme" developed by Hervé and Zaoui (1993, 2002). This homogenisation model gives an estimation of the effective properties of such composite materials and the possibility to post-process the mean value of the mechanical fields applying in each phase. Implemented into CAST3M, the CEA's finite element software dedicated to structural mechanics, this model is suitable to perform simulations on structures like nuclear fuel assemblies. To validate our model in the frame of its industrial application, we achieve finite element computations on a structure representing a part of a nuclear assembly cross-section. In this structure, the particles and the matrix are meshed to perform a reference solution of its overall thermomechanical response under nominal loading. The comparisons achieved between this reference solution and the one given by the model show the pretty good accuracy of our modelling to describe the thermomechanical behaviour of such composite materials.

Keywords: thermomechanics, modelling, homogenisation, fuel particle, HTR, GFR.

1. INTRODUCTION

In the frame of the Generation IV international forum, new concepts of nuclear reactors are investigated to provide in a few decades the technologies that would help us to face the coming century's energy problems. Among these concepts, High (or Very High) Temperature Reactors (HTR or VHTR) and Gas-cooled Fast Reactors (GFR) may share a common nuclear fuel design based on nuclear fuel particles. HTR using fuel particles is not a new concept. This kind of reactors has been developed since the 70's in Great Britain, the United States, Germany, Japan and more recently China. In order to deal with high temperatures, the nuclear fuel assembly design mostly involves ceramic materials. In addition to a better thermodynamic efficiency provided by high temperatures, HTR core components should also limit fission product release, mostly owing to the fuel-particle concept, which provides a first barrier of local containment. However the aim of developing even more efficient reactors lead us to reconsider the previous designs.

The major difficulty we face is to deal with the various scales of the problem. Fig. 1 illustrates these scales. The picture given Fig. 1 (a) represents a typical nuclear fuel assembly geometry, which dimensions are usually about 1 meter high and a few 10th of centimetres width for the hexagon side. This assembly is made up of coated

fuel particles embedded in a ceramic matrix, as illustrated Fig. 1 (b). The diameter of these particles is about 1 millimetre and the thickness of their layers about some 10^{th} of micrometers. Their size can be appreciated on the picture given Fig. 1 (c). The composition of this nuclear fuel composite material is part of the design. As a consequence, the definition of such a system is not only driven upon parameters defined at the scale of the assembly (inlet and outlet coolant temperatures, gas pressure in the channels, etc.), but also at the one of its constitutive material microstructure (volume fraction of particle, thickness of layers, material choices for the different phases, etc.), ranging scales from some 10^{th} of micrometers to 1 metre. Since such an assembly involves hundreds of millions of particles, there is no way to take explicitly into account all the details of its microstructure. The only mean to proceed is to make the link between the material composition and its *effective thermomechanical properties*.

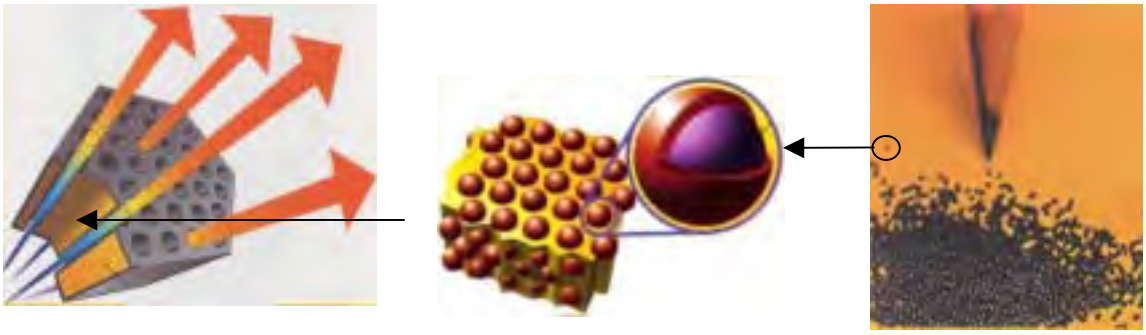

(a) *(b)* *(c)*

Fig. 1 – Illustrations of a HTR (or a GFR) nuclear fuel assembly (a) and of its constitutive material made up of spherical particles embedded in a ceramic matrix (b). Picture of coated fuel particles (c). Pictures published by the CEA (2003).

Homogenization theory in the field of thermomechanics has developed, especially since Eshelby (1957), several models which can be useful to estimate the effective properties of inclusion-based composite materials. In particular Hervé *et al.* (1993, 2002) developed the "n-layered inclusion-based self-consistent scheme", which provides the effective thermomechanical properties of composite material made up of multi-coated spherical particles embedded in a continuous matrix. More precisely, in the field of linear thermoelasticity, this model gives analytical, or semi-analytical, expressions of the effective stiffness, thermal conductivity, thermal expansion coefficient and specific heat according to those of the different phases and their relative proportions. The main interest of such a modelling is to integrate directly into the constitutive law of the material parameters connected to its composition. This model has been implemented into CAST3M, the finite element software developed by the CEA to compute structural mechanics. We then achieved a useful tool to perform simulations on nuclear fuel assemblies of HTR (or GFR).

The next section presents the homogenization model. It also gives some explanations about the way our modelling takes into account irradiation-induced deformations, and lists the relations between strains and stresses at the scale of the structure and their mean values in each phase of the composite. The third section of this article deals with the validation of our modelling in the frame of its industrial issue. This validation step is based on finite element computations of the thermomechanical fields induced in a part of a nuclear assembly cross-section. Since the mesh of this sub-structure details the matrix/particle heterogeneity, the validation consists in comparing the results obtained on the heterogeneous structure and those got on the same mesh, using the effective thermomechanical properties given by the model. The last section finally summarizes the main results of this work.

2. CHANGE SCALE MODELLING

The homogenization model we used is the result of developments initiated by Hashin and Shtrikman (1961,1962,1963), who first gave bounds for the elastic moduli of inclusion-based materials and an estimation of their effective bulk modulus. Later, Christensen and Lo (1979) proposed the first rigorous estimation of the elastic shear modulus of such materials according to the so-called "three-phase model". This model gives an estimation of the effective elastic stiffness of composite material made up of *homogenous spherical inclusions* embedded in a continuous matrix. The three-phase model has been generalised to *n-layered spherical inclusions* by Hervé and Zaoui (1993). Christensen (1979) also gave an estimation of the effective thermal conductivity and expansion coefficient according to the three-phase model. These effective properties and the effective specific heat of multi-coated inclusion-based material were finally derived by Hervé (2002).

For the sake of simplicity, we first present the three-phase model. Fig. 2 shows the representation given by this model of the material-microstructure heterogeneity. This representation is based on a *composite sphere* (the inclusion surrounded by a layer of matrix) embedded in an infinite *Equivalent Homogeneous Media* (EHM), which have the effective properties we are looking for. In the composite sphere, the radius of the matrix layer is chosen to ensure the phase proportions to be the same as in the material. Substituting this representation for the real heterogeneous microstructure, the *microscopic* thermomechanical fields induced in the two phases of the composite sphere by a given *macroscopic* thermomechanical field applying in the EHM can be determined. Once known these microscopic fields, we can then look for an equivalent homogeneous media which should behave as this heterogeneous pattern under the same thermomechanical conditions. Equivalence between the two media is generally set according to energetic criteria. In the field of *linear thermoelasticity*, this leads to analytical expressions of the effective properties: (shear (μ^h) and bulk (κ^h) elastic moduli, thermal conductivity (λ^h) and expansion coefficients (α^h), specific heat (C^h)) according to those of the two phases ($\{\mu_i,\mu_m\}$, $\{\kappa_i,\kappa_m\}$, $\{\lambda_i,\lambda_m\}$, $\{\alpha_i,\alpha_m\}$, $\{C_i,C_m\}$) and their relative proportions($\{c_i,c_m\}$). The "n-layered inclusion-based model" is easily derived from this one by substituting the homogeneous inclusion by the coated one. However, expressions for the effective properties are no longer explicit in this case. Readers interested in the details of this modelling can refer to the above references.

Fig. 2 – Heterogeneous pattern representing the material-microstructure heterogeneity according to the three-phase model. N-layered inclusion-based model is derived from this one by substituting the homogeneous inclusion by the heterogeneous one.

The effective properties are useful to simulate the response of a particle-based nuclear fuel structure to a given thermomechanical loading with no longer referring to its detailed composition. However, since each component usually undergoes shrinkage or swelling under radiation, the composite material should also exhibit a residual radiation-induced strain without any external loading. To model this radiation-induced behaviour, we consider the shrinkage or the swelling of the different phases as a set of stress-free hydrostatic strains ($\{\underline{\underline{\varepsilon}}_i^{\,f}\}_{1\le i\le n}$). For a given set of such microscopic strains, we then calculate the residual macroscopic strain ($\underline{\underline{E}}^f$) and the set of elastic strains induced in the phases due to the strain incompatibilities ($\{\underline{\underline{\varepsilon}}_i^{\,f,e}\}_{1\le i\le n}$). This last set is needed to post-process the mechanical fields in each phase.

The mean values of the strains and stresses in the kernel, in the different layers of the particle and in the matrix are linearly dependent on a given state of strains and stresses at the macroscopic scale, i.e. in the EHM. Linear operators can then be defined to post-process the mean values of the local fields. In particular, let $\mathbb{A}_i$ be the 4th-rank localisation tensor of the mean elastic strain in the ith phase of the composite. In the frame of linear elasticity, this operator gives straight fully the mean value of the strain field $\underline{\underline{\varepsilon}}_i$ according to the macroscopic one $\underline{\underline{E}}$ ($\underline{\underline{\varepsilon}}_i = \mathbb{A}_i : \underline{\underline{E}}$). However, this relation is a more complicated since the material involves locally and globally thermal expansion and radiation-induced strains. This finally leads to the following relation:

$$\forall\, i\in[1,n], \qquad \underline{\underline{\varepsilon}}_i = \mathbb{A}_i : (\underline{\underline{E}} - \underline{\underline{E}}^{th} - \underline{\underline{E}}^{f}) + \underline{\underline{\varepsilon}}_i^{th,e} + \underline{\underline{\varepsilon}}_i^{f,e} \,, \tag{1}$$

where:

- $\underline{\underline{\varepsilon}}_i$ is the mean value of the microscopic strain tensor in the ith phase,
- $\mathbb{A}_i$ is the 4th-rank localisation tensor for the ith-phase,
- $\underline{\underline{E}}$ is the macroscopic strain tensor,
- $\underline{\underline{E}}^{th} = (\lambda^h.\Delta T)\,\underline{\underline{1}}$[1] is the macroscopic thermal expansion tensor,
- $\underline{\underline{E}}^{f}$ is the macroscopic radiation-induced strain tensor,
- $\underline{\underline{\varepsilon}}_i^{th,e}$ is the microscopic elastic strain tensor in the ith phase induced by the incompatibilities of thermal expansion in the microstructure,
- $\underline{\underline{\varepsilon}}_i^{f,e}$ is the microscopic elastic strain tensor in the ith phase induced by the incompatibilities of radiation-induced strains in the microstructure.

The constitutive law of each phase then gives the stress field:

$$\forall\, i\in[1,n], \qquad \underline{\underline{\sigma}}_i = \mathbb{C}_i : (\underline{\underline{\varepsilon}}_i - \underline{\underline{\varepsilon}}_i^{th} - \underline{\underline{\varepsilon}}_i^{f}) \,, \tag{2}$$

where:

- $\underline{\underline{\sigma}}_i$ is the mean value of the microscopic stress tensor in the ith phase,
- $\mathbb{C}_i$ is the 4th-rank stiffness tensor of the ith-phase,
- $\underline{\underline{\varepsilon}}_i^{th} = (\lambda_i\,\Delta T)\,\underline{\underline{1}}$ is the thermal expansion strain tensor in the ith phase,
- $\underline{\underline{\varepsilon}}_i^{f}$ is the radiation-induced strain tensor in the ith phase.

This modelling implicitly involves several assumptions. First the temperature is supposed to be uniform at the local scale, i.e. in the composite sphere. As a consequence the thermal expansion can be supposed uniform in each phase. This is justified when the temperature gradient is weak at the scale of the microstructure. Second the radiation-induced stress-free strains are also supposed to be uniform in each phase. As for the temperature, it means that the neutron flux gradient is weak at the scale of the microstructure. These two assumptions enable to deal with the mean values of the local stress and strain fields in the expression of the local behaviour (2).

This modelling has been implemented into CAST3M. Procedures are available to compute the effective thermomechanical properties according to the model equations. These properties can be then attributed to any structure made up of a particle-based material and simulations can be achieved. Macroscopic radiation-induced stress-free strains are derived from the microscopic ones, which are part of the loading. Once the simulation done, the local fields can be post-processed. The components of the localisation tensors ($\{\mathbb{A}_i\}_{1\le i\le n}$) are given by the same procedures, as well as the thermal expansion and radiation-induced elastic strains ($\{\underline{\underline{\varepsilon}}_i^{th,e}, \underline{\underline{\varepsilon}}_i^{f,e}\}_{1\le i\le n}$). The derivation of the expressions giving these last quantities should be soon published.

3. VALIDATION OF THE MODEL

3.1. Presentation of the validation test

The validation step is based on finite element computations achieved on a structure where the material microstructure heterogeneities (the particles into the matrix) are represented. First, giving to each phase their own properties, we compute a *reference solution* for the thermomechanical response of this structure to a given loading. Next, an *homogenised solution* is calculated by attributing to all the structure the effective properties

[1] $\underline{\underline{1}}$ is the 2nd-rank identity tensor.

given by the model. The validation finally consists in comparing the temperature and the mechanical fields between these two solutions. To make the link with the underlying industrial issue, we developed the finite element mesh shown in Fig. 3. This mesh represent a part of a hexagonal-shaped fuel assembly cross-section. For a better understanding what it is, we put in the bottom left corner of the figure a drawing showing the hexagonal path of the cooling channel layout. As one can see, the meshed structure is a slice of the half triangle of composite material joining two channels. Reported dimensions are helpful to appreciate the scale of this modelling. The thickness of the slice is about 790 micrometers. The heterogeneity between the matrix and the particles was built according to a half hexagonal close-packed (hcp) cell repeated all over the structure. The volume fraction of particles in this half cell is 60%. Special care was taken on the meshing of the backward boundary and those corresponding to the channels. In particular, particles intercepting the boundaries are converted into matrix when periodicity considerations does not allow to preserve their spherical shape. Thus, even though the volume fraction of particles is locally of 60%, the remaining value is about 48%. This put into evidence the difficulty to fill such a volume with a high particle-to-matrix ratio. Finally particles are supposed to be homogeneous.

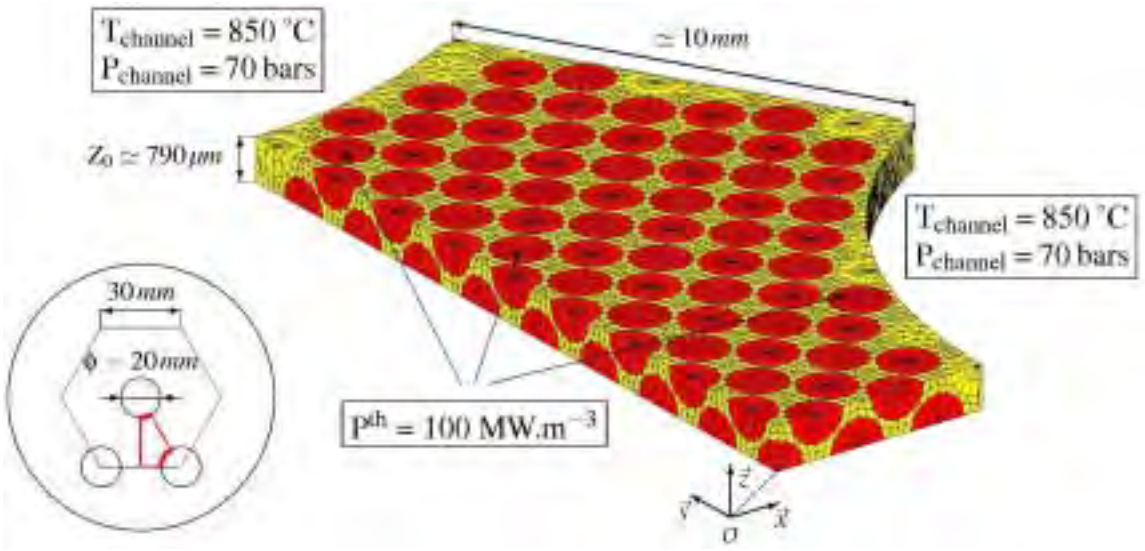

Fig. 3 – Mesh of a part of a hexagonal-shaped fuel assembly cross-section.

A local frame of coordinates is printed on the figure. Its origin, centred on the bottom corner of the mesh, has been shifted to put its axes into evidence. The particles are supposed to be made up of a mixed oxide of uranium and plutonium with 20% of plutonium. Matrix is considered to be made up of silicon carbide. The thermomechanical properties of these materials as well as their swelling and shrinkage behaviour are taken from two CEA's internal reports (Pelletier *et al.*, 2003). Some of the boundary conditions and loading are given on Fig. 3. The thermal and mechanical boundary conditions applied on the structure are:

- Thermal boundary conditions: temperature of the channel faces is set to 850°C. The thermal power of the particles, which appear in red on the figure, is set to 100MW.m^{-3}. No other boundary condition is applied on the mesh. This implies that all the heat produced by this structure is exhausted through the channels.
- Mechanical boundary conditions: nodes of the (O,x,y) plane are constrained to stay in the same plane. The same constraint is applied to the nodes of the (O,y,z) and (O,z,x) planes. The nodes of the (Z_0,x,y) plane can move upon the z-axes, but are constrained to stay in a plane of identical z-coordinate. This last boundary condition is equivalent to a generalized plane strain condition. The other faces of the mesh are displacement-free. This implies that the structure is free to expand in all directions. Finally, pressure into the channels is set at 70 bars.

3.2. Temperature field analysis

Figure 4 (b) shows temperature profiles for the reference solution (crosses) and the homogenised one (lines) along the three paths shown in Fig. 4 (a). The main interest to post-process the temperature along these paths is motivated by the global heterogeneity of the heat sources in the heterogeneous problem. Actually if you look to the mesh on figure 3, you will see that it is made up of a regular stack of half hcp cells along the line L1. Consequently the volume fraction of particles along this line should be almost the one of the cell, *i.e.* 60%, and then higher than its mean value over the mesh (48%). On the contrary, due to the elimination of several particles cut by the boundary along the line L3, the particle density along this line is certainly lower. Since the particles are heat sources, this leads to the conclusion that thermal power density is higher along the line L1 than along the line L3. Line L2 was chosen to be between L1 and L3, assuming that the power density along this line should be between these two extrema, and consequently close to its mean value over the mesh. In order to avoid any confusion, we do specify the power density in the homogeneous calculus, which is set to 48MW.m^{-3}, since the power density of one particle is 100MW.m^{-3} and the mean value of the volume fraction of particles is 48%.

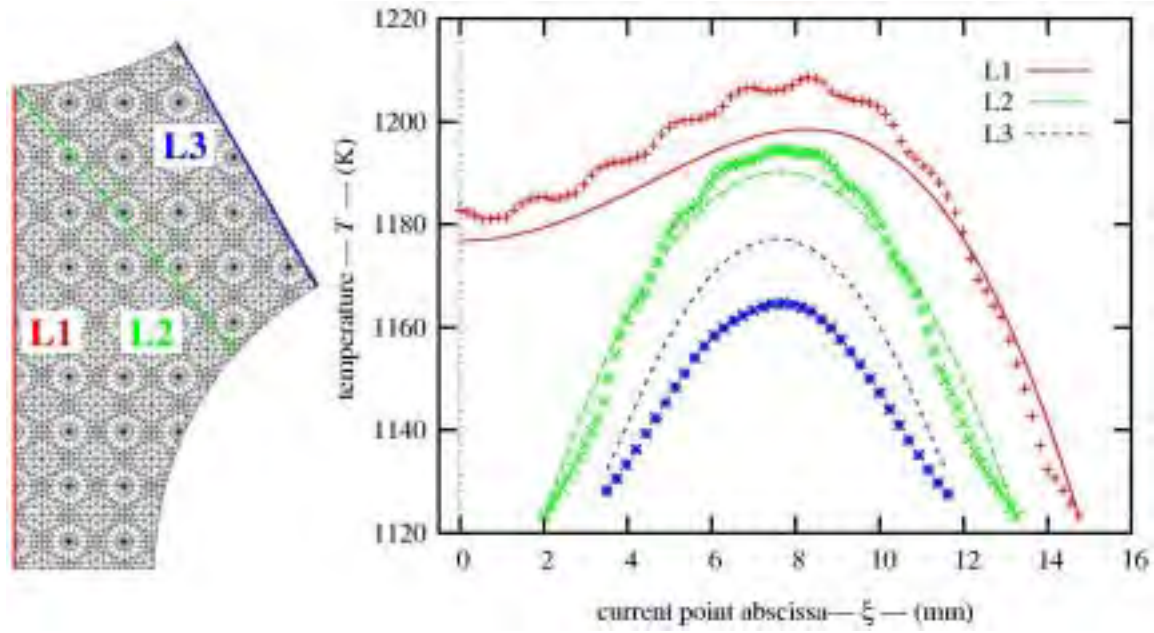

(a) (b)

Fig. 4 – Illustration of the three paths along which the temperature was post-processed (a). Temperature profiles along these three paths for the reference (crosses) and the homogenised (lines) solutions (b).

The diagram given figure 4 (b) shows the results. Temperature computed using the model matches rather well the solution along the path L2. Moreover the results along the paths L1 and L3 are in a good agreement with our analysis of the global heterogeneity of the power density, although the temperature solution is significantly higher than the one given by the model along the path L1, and lower along the path L3. Whatever this fact, the model shows a good ability to describe the thermal behaviour of such a composite material. This is particularly satisfying since these computations involve temperature and radiation-level dependent properties for which the model was not designed to. We finally notice that temperature variation across the mesh is about 100°C.

3.3. Mechanical field analysis

Fig. 5 presents the initial mesh (black) and its deformed shapes for the reference (red) and the homogenised (green) solutions. These deformed shapes are displayed with a displacement magnification equal to 10. As one can observe, they can hardly be distinguished from one to another. This indicates that the displacement fields of the two solutions are almost the same, thanks to the initial mesh to enable the comparison. According to this, the model seems accurate to describe the overall mechanical behaviour of such a composite material. Considering the problem of structural mechanics itself, the structure behaves as a free body under thermal expansion, which

is directly linked to the specified boundary conditions. However it does not imply that the structure cannot undergo any mechanical damage under such conditions. Internal stresses may play a major role since thermal expansion is strongly different between the two phases. Moreover this leads to wonder about the state of internal stresses at initial temperature in such a material, since this kind of composites is processed at high temperatures.

Fig. 5 – Mesh in its initial configuration (black) and deformed shapes for the reference (red) and homogenised (green) solutions (red mesh hardly appears since the two deformed shapes are almost the same).

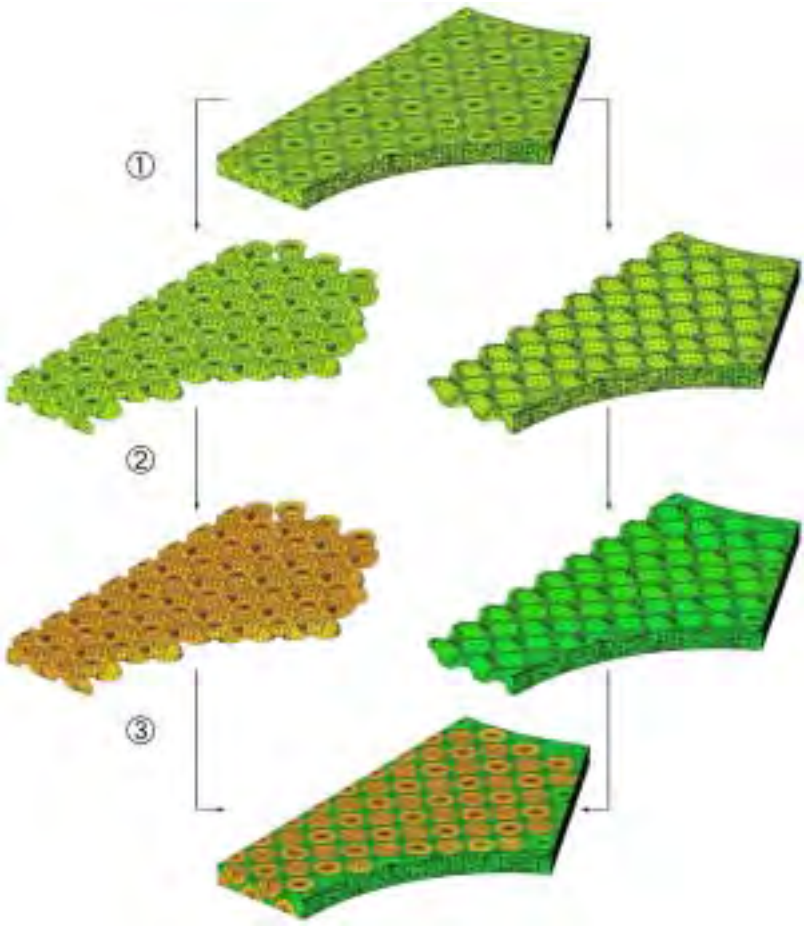

Fig. 6 – Building an estimation of the heterogeneous hydrostatic strain field from the homogenised solution and the relations of localization.

Fig. 6 illustrates how to build an estimation of any heterogeneous mechanical field from the homogenised solution and the relations of localization. As shown on the figure, this involves three steps:

① The overall homogeneous solution is reduced to the particle and matrix sub-meshes.
② On each sub-mesh, the relations of localization (1) and/or (2) are applied to determine an estimation of the mechanical field in each phase.
③ These estimations are finally joined together.

This rebuilding is only possible since the mesh we used get the two sub-meshes of the particles and the matrix. The later use of the model on structures where the material heterogeneity will no longer be meshed could also involve strain or stress localisation, but without the possibility to assemble the different solutions to built a representation of the heterogeneous one.

Thus, we also post-processed estimations of the heterogeneous stress field. Fig. 7 shows the values of the hydrostatic stress field of the reference solution (a) and an estimation built from the homogenised solution using the localisation method (b). The range of variation is very important, from –800 to 1000MPa. This is not surprising in the frame of thermoelasticity for particles behaving an important thermal expansion embedded in a very stiff matrix. When comparing the two solutions, we note that the compressive stress state in the particles is well estimated by the model. Concerning the matrix, the reference solution shows that the tensile stress state between two particles is strongly heterogeneous, ranging from about 100 MPa up to 1000MPa. On the contrary, the estimation given by the homogenised one is almost homogeneous in the inter-particle space, its value being about 500MPa. This last result is the consequence of one of the limits of the model, which only gives an estimation of the mean value of strains and stresses in each phase. However, this mean value seems correctly estimated since it appears to be in the middle of the range of variation for the reference solution.

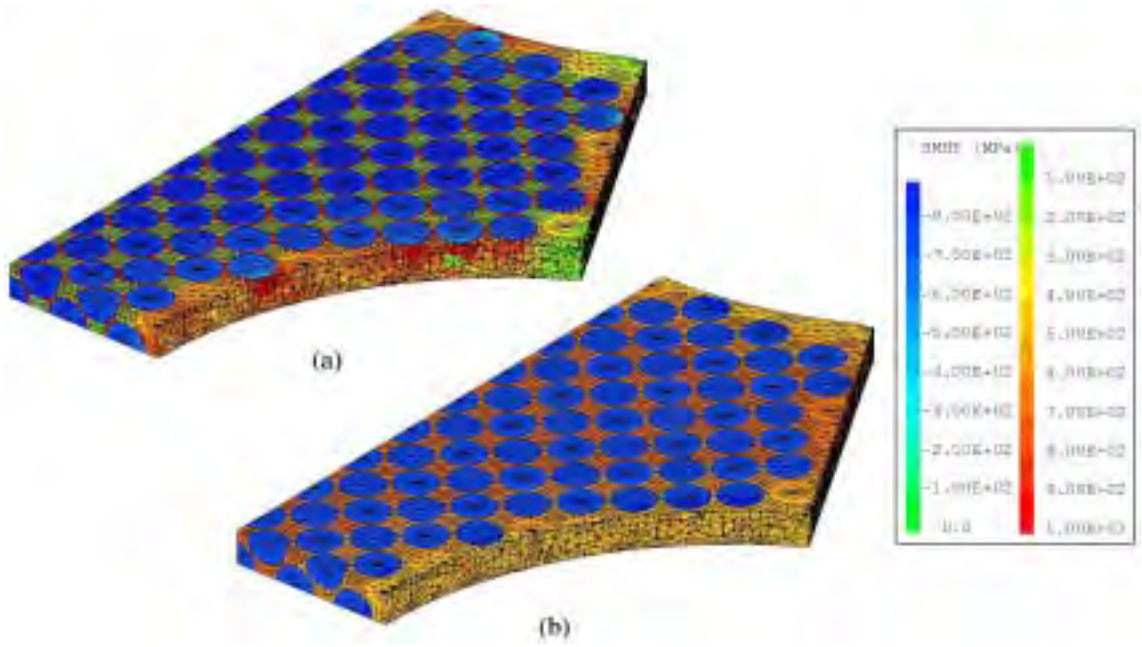

Fig. 7 – Hydrostatic stress field for the reference solution (a) and the homogenized one (b).

The analysis of the stress deviator even more highlights the local heterogeneity of the mechanical fields. Fig. 8 shows the values of the von Mises stress for the reference solution (a) and the homogenised one (b). For the former solution, the von Mises stress reaches very high values, specially in the ligament of matrix where the particles are very close. On the contrary, the von Mises stress is almost zero all over the mesh for the homogenised solution. This difference is explained by the strong heterogeneity of the stress deviator field in the inter-particle space for the reference solution, which is not estimated by the homogenised one. Fig. 9 help us to explain this result.

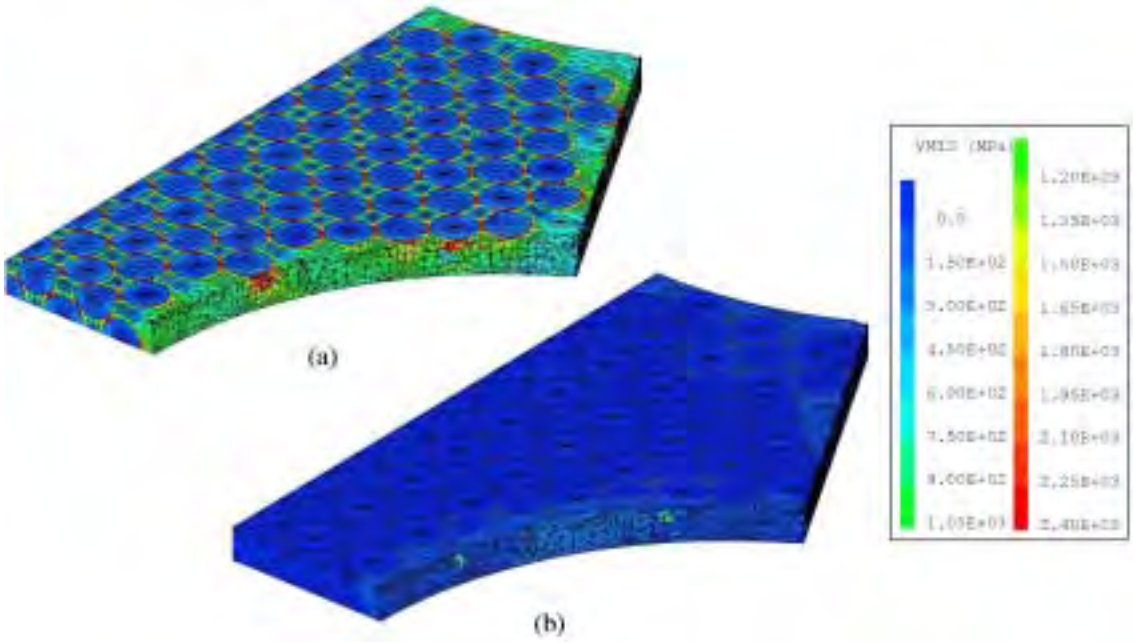

Fig. 8 – Von Mises stress field for the reference solution (a) and the homogenised one (b).

Fig. 9 shows the values of the σ_{xy} component of the stress deviator obtained for the reference solution. It can be

seen that strong shear stresses take place into the ligament of matrix joining the closest points between two particles. Moreover their values are opposite in orthogonal directions, ranging from –1000 MPa to +1000 MPa. This holds for the σ_{yz} and σ_{zx} components. The von Mises stress being a measure of the square stress deviator, it then reaches its highest values in these ligaments independently of the directions. On the contrary, the homogenised solution gives an estimation of the stress deviator averaged over the matrix layer surrounding the inclusions, as described by the pattern given Fig. 2. Since the stress deviator components take opposite values in this layer, its mean value is therefore almost zero, and so for the von Mises stress. To make it more evident, we calculated the mean value of the stress deviator components of the reference solution and displayed the von Mises stress of this new field.

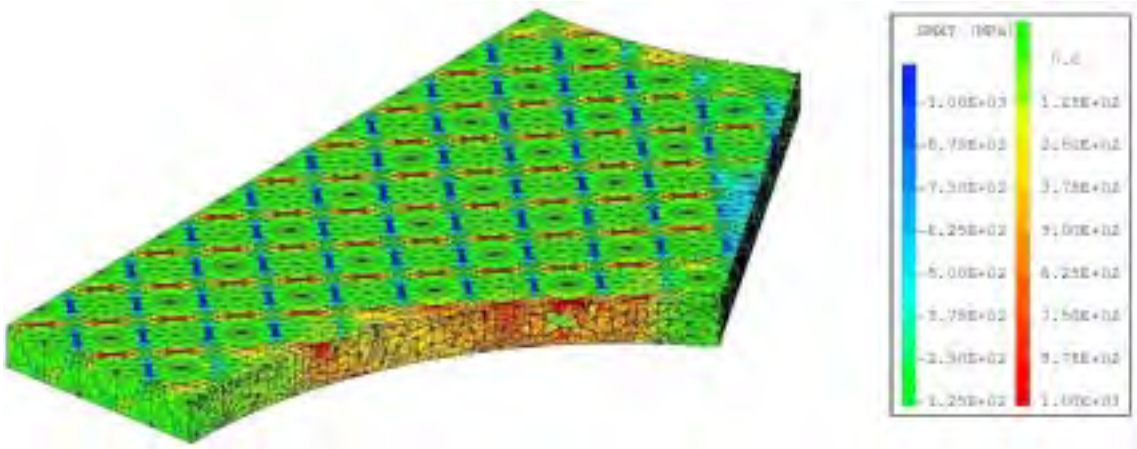

Fig. 9 – Values of the σ_{xy} component of the stress deviator for the reference solution.

Fig. 10 shows the von Mises stress of the stress deviator averaged all over the matrix sub-mesh for the reference (a) and the homogenised (b) solutions. It can be noticed that these two fields are now closer than before. The value of the reference solution obtained by this way is about 50 MPa, while the estimated one is about 70 MPa. This first demonstrates that the mean values of the stress deviator components are actually very weak compared to their extremes. Second it clearly shows that the model gives good estimations of the required quantities such as the values of the mechanical fields averaged over the volume defined by the matrix layer considered in the pattern of the Fig. 2.

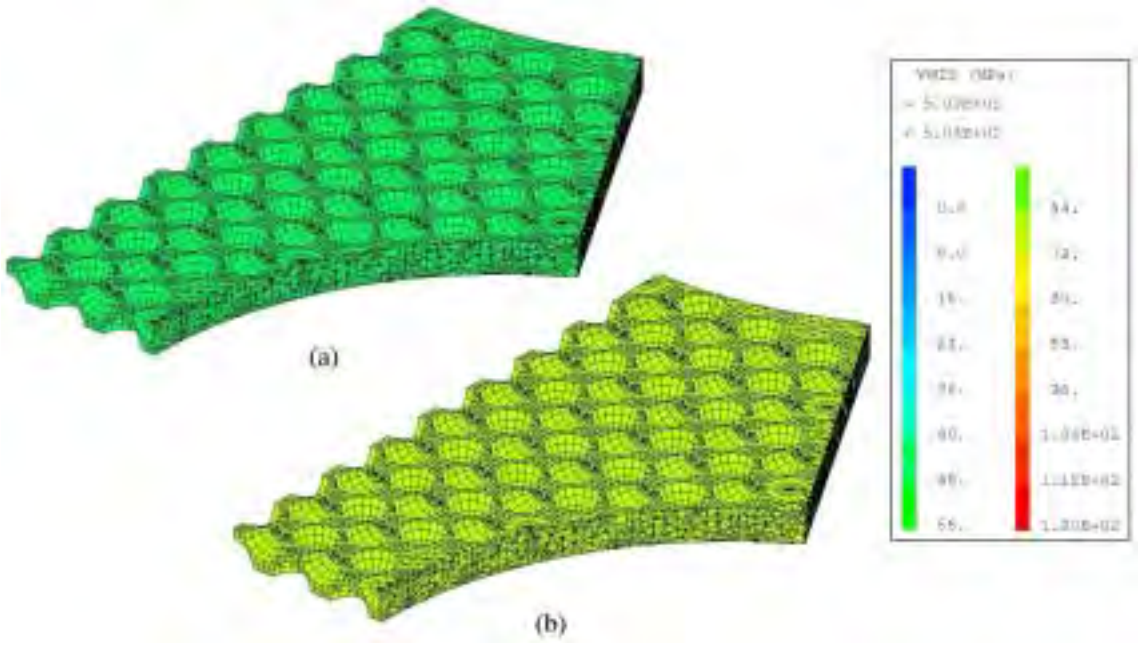

Fig. 10 – Von Mises stress of the stress deviator averaged all over the matrix sub-mesh for the reference solution (a) and the homogenised one (b).

4. CONCLUSIONS

On the basis of the "n-layered inclusion-based self-consistent scheme" (Hervé and Zaoui, 1993, 2002), we developed a change scale modelling of the thermomechanical behaviour of particle-based nuclear fuel materials. In the one hand this model provides their effective thermomechanical properties, which are helpful to perform finite element computation on structures made up of such composite materials. On the other hand it also gives the possibility to post-process the mean values of the local mechanical fields, which apply in each of its phases. CAST3M procedures have been finally developed to make the model available into the CEA's finite element software.

In order to check the ability of this model to describe the thermomechanical behaviour of such nuclear fuels in the frame of the industrial issue, we achieved comparisons between the thermal and mechanical fields computed on a structure representing a part of a cross-section of a nuclear fuel assembly under nominal loading. These comparisons lead to the following main results:

- The homogenised solution offers a good description of the temperature field, with a temperature variation over the structure of about 100°C.
- The overall thermomechanical behaviour is also well reproduced, with a good estimation of the displacement field over the structure.
- Localised stress and strain fields in each composite phase match with a good accuracy their mean value in the reference solution. However the strong heterogeneity of the mechanical fields into the matrix phase cannot be handle by the model. This will certainly be a problem when trying to push this modelling towards non-linear behaviour.

We are also satisfied to obtain these results for temperature-dependant material properties since this model was only developed in the frame of *linear* thermoelasticity. Of course this only holds for the current thermal and mechanical loadings. Care should be taken when using this modelling in the frame of stronger thermomechanical gradients, like in transient loadings for example.

REFERENCES

CEA, (2003), Les défis du CEA, No. 95, pp. 22-25 (in french).

Christensen, R.M., Lo, K.H., (1979), J. Mech. Phys. Solids, Vol. 27, pp. 315-330.

Christensen, R.M., (1979), Mechanics of composite materials, Wiley Interscience, New York.

Eshelby, J.D., (1957), Proc. Roy. Soc., A241, pp. 376-396.

Hashin, Z., (1962), J. Appl. Mech., Vol. 29, pp. 143-150.

Hashin, Z., Shtrikman, S., (1961), J. Franklin Inst., Vol. 271, pp. 336-341.

Hashin, Z., Shtrikman, S., (1963), J. Mech. Phys. Solids, Vol. 11, pp. 127-140.

Hervé, E., Zaoui, A., (1993), Int. J. Engng. Sci., Vol. 31, No. 1, pp. 1-10.

Hervé, E., (2002), Int. J. Solids Struc., Vol. 39, pp. 1041-1058.

Pelletier, M., Nabielek, H., Abram, T., Martin, D., (2003), Internal report CEA/DEN/CAD/DEC/SESC/LSC 03-028.

Pelletier, M. ,Martin, D., (2003), Internal report CEA/DEN/CAD/DEC/SESC/LSC 03-029.

